Journal of Alloys and Compounds, 207/208 (1994) 14–19
JALCOM 3006

The use of gadolinium and dysprosium chelate complexes as contrast agents for magnetic resonance imaging

Alan D. Watson
Nycomed Salutar, Inc., 428 Oakmead Parkway, Sunnyvale, CA 94086 (USA)

Abstract

Polyaminopolycarboxylic acid complexes of gadolinium are now finding widespread application as magnetic resonance contrast agents based primarily upon their ability to alter T_1 and T_2 relaxation rates *in vivo*. Both gadolinium and dysprosium complexes are also beginning to be utilized as T_2^*, or magnetic susceptibility contrast agents, to image perfusion in the human heart and brain or to enhance contrast in functional and perfusion imaging applications. The ability of a lanthanide to produce this effect is related to the square of its magnetic moment; dysprosium complexes ($\mu = 10.6$ BM) appear optimal for this application and are likely to have major advantages in the clinical setting. The properties of the gadolinium and dysprosium complexes that are currently, or have been, under investigation as either relaxation-based or susceptibility agents (or both) are discussed. Particular attention is paid to the ligand type, acyclic or cyclic, since this is a major determinant of the physicochemical and biological properties of these complexes. The physicochemical characterization and development of a new nonionic dysprosium complex, DyDTPA-BMA (Sprodiamide), as a heart and brain imaging agent is described.

1. Introduction

The utility of chelate complexes of lanthanides to enhance contrast in MR images, through their ability to differentially alter T_1 and T_2 relaxation rates of protons in tissue through which they pass, is now well established. $(NMG)_2Gd(DTPA)$* has been used clinically for this purpose for over 5 years [1] to assist in the diagnosis of a variety of CNS lesions of the brain and spine. Newer, potentially safer non-ionic complexes such as Omniscan™ (GdDTPA-BMA) and ProHance™ (GdHPDO3A) have recently been approved in the United States and the United Kingdom for similar applications [2,3].

In addition to their considerable T_1 and T_2 relaxivities, which allow them to function as relaxation enhancers (providing an increase in signal intensity), gadolinium complexes have a magnetic moment of 7.6 BM. This enables them to also function as effective magnetic susceptibility, or T_2^*, contrast agents, able to reduce signal intensity due to their ability to induce a loss of proton phase coherence (negative enhancement) in tissues through which they pass [4]. Dysprosium complexes have a negligible T_1 relaxivity due to their extremely fast electron spin relaxation times. However, dysprosium has a magnetic moment of 10.6 BM, the highest of all the lanthanides, which makes it the most effective T_2^* susceptibility contrast agent amongst this class of materials [5].

A variety of ligands have been used to generate contrast-enhancing metal chelate complexes of gadolinium and dysprosium. Such ligands include both acyclic and cyclic polyaminopolycarboxylates [6]. In the following sections, representative examples of both gadolinium and dysprosium complexes of these ligands and their utility as MR contrast agents are described.

*Abbreviations: BOPTA, (benzyloxymethyl)diethylenetriaminepentaacetic acid; DO3A, 1,4,7,10-tetraazacyclododecane-*N*,*N*′,*N*″-triacetic acid; DOTA, 1,4,7,10-tetraazacyclododecane-*N*,*N*′,*N*″,*N*‴-tetraacetic acid; DTPA, diethylenetriaminepentaacetic acid; DTPA-BMA, diethylenetriaminepentaacetic acid bis(methylamide); DTPA-EOB, (ethoxybenzyl)diethylenetriaminepentaacetic acid; EDTA, ethylenediaminetetraacetic acid; HEDTA, hydroxymethylethylenediaminetriacetic acid; HP-DO3A, 10-(2′-hydroxypropyl)-1,4,7,10-tetraazacyclododecane-*N*,*N*′,*N*″-triacetic acid; NTA, nitrilotriacetic acid; TETA, 1,4,8,11-tetraazacyclotetradecane-*N*,*N*′,*N*″,*N*‴-tetraacetic acid; TTHA, triethylenetetraminehexaacetic acid.

2. Acyclic complexes

The acyclic ligand DTPA was first prepared in 1946 [7] and its metal-binding properties rapidly established [8–10]. By 1952 [11], the usefulness of ligands such as EDTA to detoxify free metal ions was routinely exploited in vivo to alleviate heavy metal poisoning. During the

SSDI 0925-8388(93)03006-5

1970s, research [12] on the relaxation probe GdEDTA led to the use of EDTA and other linear polyaminopolycarboxylates such as DTPA and TTHA as ligands [13] to solubilize lanthanide ions over the physiological pH range and to reduce their intrinsic metal ion toxicity [14,15]. Utilizing paramagnetic lanthanides such as gadolinium and dysprosium has given rise to a class of useful, highly water soluble in vivo MRI relaxation-based contrast-enhancing agents [16,17].

Early structural studies on lanthanide chelate complexes revealed greatly varying ligand geometries and coordination numbers ranging from eight to ten [18,19]. Solid-state X-ray studies [20,21] of $Na_2GdDTPA \cdot H_2O$ and $BaNdDTPA \cdot 3H_2O$ indicated that both lanthanide ions were nine-coordinate. The central metal ion was coordinated to the three amine nitrogens and five carboxylate oxygens of the ligand to form a square antiprism around the metal atom. A single water molecule capped the large open square face of the antiprism.

The X-ray structures of both GdDTPA-BMA and DyDTPA-BMA have recently been completed [22,23] and differ in several ways from the earlier lanthanide DTPA chelate complex X-ray determinations. Both gadolinium and dysprosium coordination polyhedra are nine-coordinate tricapped trigonal prisms occupied by three amine nitrogen atoms and three carboxylate oxygen atoms, with bond lengths that are comparable to those observed in $BaNdDTPA \cdot 3H_2O$. Surprisingly, however, both amide carbonyl oxygen atoms are bound to the central metal atom. This arrangement explains, in part, the smaller than expected reduction [24] in the thermodynamic stability constant between $(NMG)_2$-GdDTPA and complexes in which two of the carboxylates are converted to amide groups (theoretically, the loss of two strongly coordinating donor atoms should produce an even greater decrease in stability). The coordination of a single water molecule within the first coordination sphere suggests that the relaxivity properties of GdDTPA-BMA would be analogous to those of $(NMG)_2GdDTPA$. This has been demonstrated in both *in vitro* relaxivity studies in water and plasma, and *in vivo* imaging studies [25].

Preclinical pharmacology and toxicology studies of $(NMG)_2GdDTPA$ [26,27] showed that *in vivo* demetallation of $(NMG)_2GdDTPA$ occurs over time accompanied by the deposition of free gadolinium ion in the liver and bone, so that applications which require a significant residence time in the body are a problem.

Thus while $(NMG)_2GdDTPA$ specifically, and gadolinium-based agents generally, are not innocuous, they do have an excellent safety profile, and the incidence of severe adverse reactions is exceedingly low. Driving forces for new agents arose from the desire to further improve existing safety profiles, and to provide low osmolal complexes so that it would be possible to safely inject higher dosages than 0.1 mmol kg^{-1} of both gadolinium and dysprosium chelate complexes, especially for potential application to dynamic and susceptibility-based MR imaging.

The first of the second-generation MRI contrast-enhancing agents, GdDTPA-BMA, was prepared by combining gadolinium with the DTPA chelate derivative, DTPA-bis(methylamide), which contains only three anionic carboxylate binding sites to neutralize the cationic charge (3+) of the gadolinium ion [28]. Since the resulting complex does not require counterions, GdDTPA-BMA and its congener DyDTPA-BMA are non-ionic complexes which give rise to low osmolal solutions.

A variety of unsubstituted and hydroxyl substituted acyclic bisamide complexes have now been evaluated, although none so far have offered sufficient improvement over the lanthanide DTPA-BMA complexes to warrant clinical development. Non-ionic gadolinium complexes have also been obtained by neutralizing the anionic charge on two of the DTPA carboxylate groups through functionalization with ester groups [29]. Since these gadolinium complexes are subject to hydrolysis, however, further development has not been pursued.

The remaining, readily available, acyclic polyaminopolycarboxylates include EDTA, TTHA and NTA. The gadolinium complexes of all three ligands have been evaluated as contrast-enhancing agents. GdEDTA (LD_{50} (rats) = 0.3 mmol kg^{-1}) is even more toxic than $GdCl_3$ (LD_{50} (rats) = 0.5 mmol kg^{-1}) [30] and this complex has the potential to labilize gadolinium [24] ($\log K_{therm} \sim 17$; $\log K_{sel} \sim 4.28$) for distribution to a wide variety of sites *in vivo*, primarily bone. $GdCl_3$, on the other hand, rapidly forms insoluble hydroxide particulates that aggregate in the liver and release gadolinium only slowly [31].

GdTTHA has an acceptable toxicity profile. However, the ligand is a nonadentate chelate in which three backbone amines and six carboxylates act as donors, and so the complex is coordinatively saturated. As a result, the first coordination sphere of the gadolinium complex contains no labile water molecules, and its relaxivity is approximately half that of $(NMG)_2$-GdDTPA or GdDTPA-BMA. The calculated selectivity constant (K_{sel}) for GdNTA is 4.15 and for the gadolinium complex of HEDTA is 5.02. Both constants are low compared to those of GdDTPA-BMA (9.0) and GdDTPA (7.0), and significant *in vivo* metal exchange and ligand exchange readily occurs. For these reasons, GdNTA, GdHEDTA and GdEDTA are considered much too toxic for clinical applications.

GdBOPTA, a candidate for liver imaging, is a GdDTPA derivative [32] the backbone of which contains a benzyloxymethyl group (LD_{50} (mice) = 6 mmol kg^{-1}). This substituent group is believed to provide the required

handle for the anionic hepatocyte receptor that also binds bromosulfophthalein. Its X-ray structure shows the gadolinium ion to be nine-coordinate, with one water molecule in the first coordination sphere. The aqueous relaxivities are consistent with this environment ($R_1 = 4.4\ mM^{-1}\ s^{-1}$, $R_2 = 5.6\ mM^{-1}\ s^{-1}$ at 20 MHz and 37 °).

The pharmacokinetics of GdBOPTA in animals demonstrate rapid hepatocyte uptake and excretion of 25–50% of the administered dose into the bile [33] while the remainder is excreted in the urine. GdBOPTA is apparently excreted unmetabolized, although subchronic toxicity data and complete metabolism studies have not yet been reported. GdBOPTA appears to be highly efficacious in animals; the reduction in $T1$ it produces is significant, and hepatic signal intensity increases. Since liver tumors show little uptake of the drug, liver-to-tumor image contrast is greatly increased for T_1-weighted images [34].

A second potential gadolinium-based chelate for hepatobiliary imaging is GdDTPA-EOB, a derivative of GdDTPA containing a lipophilic ethoxybenzyl group on the backbone. Hepatic uptake of GdDTPA-EOB is reduced by cholestasis and bromosulfophthalein infusion suggesting transport via the hepatocyte organic anion receptor [35]. The biodistribution by GdDTPA-EOB is primarily hepatobiliary (*ca.* 63%) with the balance excreted in urine [36]. The metabolic profile is yet to be reported, however. A dose of 0.1 mmol kg^{-1} GdDTPA-EOB enhanced the liver signal in rats up to 200% above background and remained at over 100% for 30 min.

The structures of several of the acyclic ligands discussed are shown in Figs. 1 and 2.

GdDTPA has been shown to improve the MRI detection of cerebral infarcts in brain regions with an eroded or deficient blood–brain barrier. However, gadolinium MRI enhancement in the acute or subacute stage of stroke has been a variable finding. The utility of extracellular T_1-based MRI contrast enhancing agents has been limited mainly by the requirement for a static intravascular concentration of the agent. Currently available agents are not able to cross the intact blood–brain barrier, and the fast exchange relaxation kinetics of water from the interstitial space into the cerebral vasculature (high concentration of T_1 contrast agent) do not appear to correlate with tissue blood flow.

Gadolinium complexes are also able to function as T_2^*, or magnetic susceptibility, contrast agents. Inhomogenously distributed contrast agents give rise to microscopic magnetic field gradients which influence MR signal intensity via so-called T_2^* relaxation or magnetic susceptibility effects. Magnetic susceptibility is the proportionality constant between the applied magnetic field strength and the resulting magnetization established in

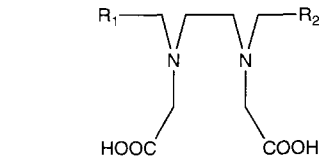

R1 = R2 = -COOH **EDTA**

R1 = -COOH, R2 = -OH **HEDTA**

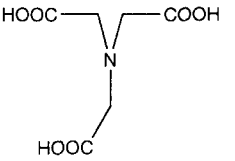

NTA

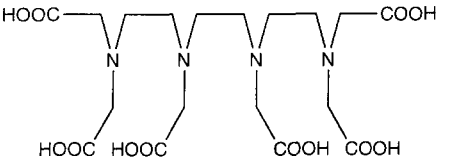

TTHA

Fig. 1. Schematic diagram of the acyclic ligands EDTA, HEDTA, NTA and TTHA.

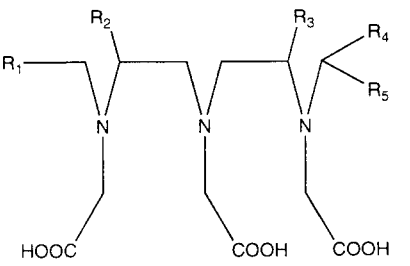

$R_1 = R_4 = -COOH$, $R_2 = R_3 = R_2 = -H$, **DTPA**

$R_1 = R_4 = -CONHCH_3$, $R_2 = R_3 = R_5 = -H$ **DTPA-BMA**

$R_1 = R_4 = -COOH$, $R_2 = R_5 = -H$, $R_3 = -CH_2C_6H_5OC_2H_5$ **DTPA-EOB**

$R_1 = R_4 = -COOH$, $R_2 = R_3 = -H$, $R_5 = -CH_2OCH_2C_6H_5$ **BOPTA**

Fig. 2. Schematic diagram of the acyclic ligands DTPA, DTPA-BMA, DTPA-EOB and BOPTA.

the tissue. A significant concentration of a magnetic susceptibility contrast agent can be compartmentalized within the intravascular space, leading to a loss of phase coherence and a pronounced reduction in signal intensity in T_2^*-weighted images, that extends beyond the vasculature into surrounding tissue parenchyma, as shown in Fig. 3. Ischemic regions remain isointense with the precontrast images, thereby clearly delineating the boundaries of hypoperfused tissues.

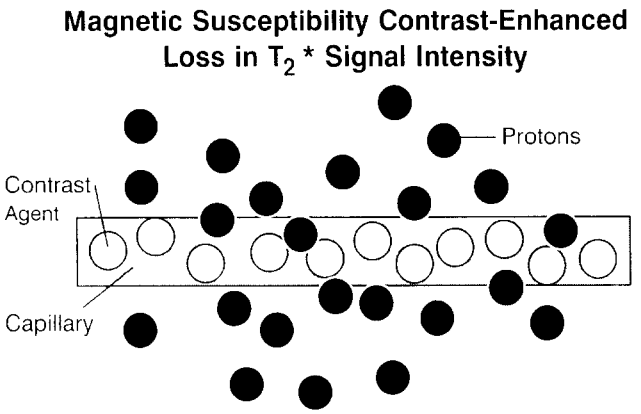

Fig. 3. Schematic figure of capillary perifusion which describes the mechanism of T_2^* contrast agent induced signal intensity loss due to water proton diffusion through capillary spaces.

Both conventional spin-echo and fast scan gradient-echo pulse sequences can be used to observe the effects of magnetic susceptibility-induced signal changes. In spin-echo imaging, regional signal intensity loss is due to the diffusion of tissue water through static field gradients next to the contrast-filled capillaries. Fast-scan techniques also permit assessment of the dynamics of compartmentalization of the agents, from which regional blood volume and tissue perfusion data can be derived.

The dependence of efficacy (signal intensity loss) on the square of the magnetic moment leads to dysprosium as the optimal choice of metal ion. Early studies [4] focused on salts of DyDTPA; however significantly higher dosages (0.5–1.0 mmol kg^{-1}) than those typically employed when using GdDTPA were required to observe useful signal intensity reduction. The decrease in the safety index (LD_{50}/effective dosage) of this complex at these high dosages (an LD_{50} in the range 5–10 mmol kg^{-1} gives a safety margin range of only 5–20) made this complex problematic for clinical development.

DyDTPA-BMA is a non-ionic paramagnetic lanthanide metal chelate complex used as an intravenously injectable T_2^* contrast agent to reduce MR image signal intensity, and hence increase visual contrast between normally and abnormally perfused tissues. When formulated with 5 mol% CaNaDTPA-BMA, a 500 mM solution of DyDTPA-BMA has a significantly improved toxicity profile (LD_{50} in the range 22–30 mmol kg^{-1}) and this agent (Sprodiamide injection) is presently in the early stages of clinical development. A number of animal imaging studies have demonstrated its efficacy as a tissue perfusion imaging agent at dosages as low as 0.1 mmol kg^{-1} in both heart and brain [5,37].

The replacement of gadolinium by dysprosium in DTPA-BMA provides an agent with a 1.8-fold increase in magnetic susceptibility properties and utility *in vivo* through detoxification of the dysprosium ion. In comparison to ionic contrast agents such as $(NMG)_2$-GdDTPA and $(NMG)_2$DyDTPA, non-ionic metal chelates have higher stability (K_{sel}), reduced osmolality at the same dosages and similar physical properties [24]. These features provide a higher usable dosage range and an increased margin of safety.

When magnetic susceptibility contrast agents are used in conjunction with ultra-fast imaging techniques, functional tissue perfusion maps can be generated. The signal intensity versus time data, based on the first pass effect of the contrast agent through the microvasculature, can be converted to concentration versus time data. Calculations of the signal intensity changes over time for each voxel can then be used to produce high-resolution, regional blood volume images. If an arterial input function is added, deconvolution analysis can be used to find the true plasma clearance, the mean transit time through the capillary network and ultimately regional tissue blood flow [38].

Clinical development of Sprodiamide Injection is moving forward. Phase I clinical trials explored the safety of this agent in normal volunteers, up to a dosage of 1.5 mmol kg^{-1}, without any significant adverse events. The efficacy of Sprodiamide Injection to reduce signal intensity in both cardiac and cerebrovascular tissue in normal human volunteers at a clinically acceptable dosage. The ability to quantify blood volume, enabling a determination of relative tissue perfusion, was also established [39,40]. Additional Phase II/III clinical trials in patients are planned to encompass a wide range of tissue perfusion applications including heart, brain, liver, kidneys and the peripheral vascular system.

3. Cyclic complexes

Ligands that combine the characteristics of higher stability with lanthanide selectivity are likely to form a good basis for improved MRI contrast-enhancing agents [41]. Polyazapolycarboxylate macrocycles function as lanthanide-specific chelates, and their thermodynamic and kinetic stability properties are superior to those of acyclic ligands such as EDTA and DTPA. The reorganization entropy associated with the incorporation of a metal decreases when a potential metal binding site within a ligand becomes more encapsulated or preformed through the use of a rigid macrocyclic structure. This reduced entropy leads to a relatively higher stability constant for metal binding observed for example, in the greater stability of GdDOTA relative to GdDTPA. This effect is termed the 'macrocyclic' or 'clathrochelate' effect [41].

Early studies [42–44] on DOTA and TETA provided a good working knowledge of the pK_a values, lanthanide

complex stability constants, and physical properties of the gadolinium complexes of these ligands.

A full X-ray crystallographic analysis of GdDOTA is not yet available, however the analogous EuDOTA complex is nine-coordinate [45]. The coordination sphere contains four amine nitrogens, four carboxylate oxygen donor atoms, and a water oxygen. The complex is conformationally rigid in the solid state and in solution, resulting in metal-binding kinetic properties that are very different from those of the acyclic chelates. The $\log K_{therm}$ of GdDOTA is in the range 25–28, as compared to 22–23 for GdDTPA. This difference [46] can be attributed to:

- a reduction in steric strain due to the formation of eight five-membered rings upon metal complexation
- the macrocyclic effect [41], which results in a 3–5 order of magnitude increase in stability over that of complexes containing acyclic ligands

DOTA, like the other polyazapolycarboxylate macrocycles, forms kinetically inert complexes. The ligand takes up metal ions extremely slowly and releases them equally slowly under competitive (*in vivo*) conditions [43] so that GdDOTA has a metal release half-life of 21 days at pH 1.5. To date (NMG)GdDOTA (gadoterate) has been used to detect a variety of cerebral and spinal lesions, at the same dose levels and with comparable efficacy to $(NMG)_2GdDTPA$.

A range of non-ionic DO3A cyclic chelate complexes have been developed to try and take advantage of the more desirable characteristics exhibited by the non-ionic acyclic gadolinium chelate complexes and cyclic ligands. Three carboxylate groups from ring nitrogens neutralize the charge of a tripositive metal ion, while the fourth carboxylate moiety is functionalized with a variety of amide, ester, and hydroxylated sidechains [47]. Fluorescence decay data indicate that 1.1 molecules of water per mole of complex are bound in the first coordination sphere [48], confirmed by a recent crystallographic analysis of the 2-hydroxypropyl derivative of GdDO3A (GdHP-DO3A or gadoteridol). GdDO3A has an osmolality of 400 mmol kg^{-1} in aqueous solution and an LD_{50} (rats, i.v.) above 10 mmol kg^{-1}. Other physicochemical, metal binding, stability and relaxivity properties of GdDO3A closely parallel those of GdDOTA [46]. The structures of the macrocyclic ligands discussed above are shown in Fig. 4.

Although the molar relaxivities and biodistribution of the extracellular gadolinium chelates GdDTPA, GdDOTA, GdDTPA-BMA, and GdHP-DO3A are very similar (detailed in Table 1), the osmolalities, *in vivo* stabilities, and toxicities (LD_{50}) of these compounds differ substantially. These differences may relate primarily to the safety index of the compound and could be significant for dosages greater than 0.1 mmol kg^{-1}, multiple doses, and for oral administration. The only cyclic complexes to date which have been explored as T_2^* contrast agents are GdDOTA at a high dosage (0.5 mmol kg^{-1}) and DyDOTA.

The now-established ability of the various gadolinium complexes to act as tissue perfusion contrast media at higher dosages is under exploration, but the limitations described earlier may reduce their utility. The development of relatively non-toxic chelate complexes such as GdDTPA-BMA and DyDTPA-BMA has enabled contrast-enhanced MRI to be utilized for an ever widening number of applications, and the advent clin-

TABLE 1. Properties of some CNS MR contrast media

	Magnevist® (gadopentatate dimeglumine)	Dotarem® (gadoterate meglumine)	Omniscan™ (gadodiamide)	ProHance® (gadoteridol)
Molecular weight (g mol^{-1} including NMG)	938	752	573	559
Charge	−2	−1	0	0
Osmolality (mOsm kg^{-1})	1940	1170	790	630
Relaxivity (10 MHz, 37 °C)				
R_1 (mM^{-1} s^{-1})	4.5	4.5	4.6	3.7[a]
R_2 (mM^{-1} s^{-1})	5.7	5.8	5.1	–
LD_{50} (mice; mmol kg^{-1})	6–10	11	34	12
Safety index[b] (0.1 mmol kg^{-1})	60–100	110	340	120

[a]20 MHz, 37 °C.
[b]LD_{50}/effective dosage.

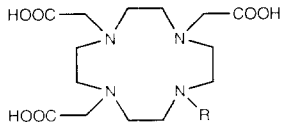

R = -CH_2COOH DOTA

R = -H DO3A

R = -$CH_2CH(OH)CH_3$ HP-DO3A

Fig. 4. Schematic diagram of the tetraaza-based macrocycles DOTA, DO3A and HP-DO3A.

ically of routine multiple and high dosage studies with a large margin of safety will expand their utility even further in the future.

Acknowledgements

The author wishes to acknowledge the assistance of Sue Wright and Ken Callahan in the preparation of this manuscript.

References

1 H.P. Niendorf, *Contrast Media in MRI*, International Workshop, Bossum, Medicom, Berlin, 1990.
2 E.S. Harpur, D. Worah, P.A. Hals, E. Holtz, K. Furuhama and H. Nomura, *Invest. Radiol. Suppl., 28* (1993) S28.
3 M. Seiderer, *Invest. Radiol. Suppl., 27* (1992) S33.
4 A. Villringer, B.R. Rosen, J.W. Belliveau, J.L. Ackerman, R.B. Lauffer, R.B. Buxton, Y.-S. Chao, V.J. Wedeen and T.J. Brady, *Magn. Reson. Med., 6* (1988) 164.
5 M.E. Moseley, J. Kucharczyk, J. Kurhanewicz, W.M. Chew, M.F. Wendland, S.M. Rocklage, S. Quay and D. Norman, *SMRM*, Abstracts, 8th Annual Meeting, Amsterdam, 1989, p. 43.
6 A.D. Watson, S.M. Rocklage and M.J. Carvlin, in D.D. Stark and W.G. Bradley (eds.), *Magnetic Resonance Imaging*, 2nd edn., Mosby, St. Louis, MO, 1992, Ch. 14.
7 F.C. Bersworth, *US Patent 2,407,645,* granted 9/17/46 (Martin Dennis Co.).
8 E.J. Durham and D.P. Ryskiewich, *J. Am. Chem. Soc., 80* (1958) 4812.
9 A.E. Frost, *Nature, 178* (1956) 322.
10 R. Harder and S. Chaberek, *J. Inorg. Nucl. Chem., 11* (1959) 197.
11 E.L. Belknap, *Ind. Med. Surg., 21* (1952) 305.
12 C.D. Barry, J.A. Glasel, R.J.P. Williams and A.V. Xavier, *J. Mol. Biol., 84* (1974) 471.
13 J.J. Dechter and G.C. Levy, *J. Magn. Res., 39* (1980) 207.
14 H. Spencer and B. Rosoff, *Health Phys., 11* (1965) 1181.
15 B. Rosoff, E. Siegel, G.L. Williams and H. Spencer, *Int. J. Appl. Radiat. Isot., 14* (1963) 129.
16 D.H. Carr, J. Brown, G.M. Bydder, R.E. Steiner, H-J. Weinmann, V. Speck, A.S. Hall and I.R. Young, *Lancet, i* (1984) 434.
17 H. Gries, D. Rosenberg and H-J. Weinmann, *German Patent Appl. DE 3,129,906,* filed July 24 1981 (Schering AG).
18 S.P. Sinha, *Struct. Bonding, 45* (1976) 69.
19 R.J.P. Williams, *Struct. Bonding, 50* (1982) 79.
20 H. Gries and H. Miklautz, *Physiol. Chem. Phys. Med. NMR, 16* (1984) 105.
21 J.J. Stezowski and J.L. Hoard, *Isr. J. Chem., 24* (1984) 323.
22 E. Ehnebom and B.F. Pedersen, *Acta Chem. Scand., 46* (1992) 126.
23 A. Watson, *3rd European Workshop on Magnetic Resonance in Medicine 1992*, Hamburg, Germany, in press.
24 W.P. Cacheris, S.C. Quay and S.M. Rocklage, *Magn. Res. Imaging, 8* (1990) 467.
25 R.N. Muller, P. Vallet, F. Maton, A. Ruch, J.F. Goudemant, L. VanderElst, P. Gillis, S. Peto, F. Moiny and Y. Van-Haverbeke, *Invest. Radiol., 25 (suppl)* (1990) S34.
26 P. Wedeking and M. Tweedle, *Int. J. Rad. Appl. Instrum. [B], 15* (1988) 395.
27 P. Wedeking, K. Kumar and M.F. Tweedle, *Magn. Reson. Imaging, 10* (1992) 641.
28 S.C. Quay, *US Patent 4,687,659,* granted 8/18/87 (Salutar, Inc.).
29 S.C. Quay, *US Patent 4,687,658,* granted 8/18/87 (Salutar, Inc.).
30 H.J. Weinmann, R.C. Brasch, W.R. Press and G.E. Wesbey, *Am. J. Roentgenol., 42* (1984) 619.
31 R.A. Ball, G. Van Gelder, J.W. Green and W.O. Reece, *Proc. Soc. Exp. Biol. Med., 135* (1970) 426.
32 P. Pavone, G. Patrizio, C. Buoni, E. Teltamanti, R. Passariello, C. Musu, P. Tirone and E. Felder, *Radiology, 176* (1990) 61.
33 F. Cavagna, P. Tirone, E. Felder and C De Haën, *2nd European Workshop on Magnetic Resonance in Medicine*, Bordeaux, France, 1991, p. 83.
34 T.J. Vogel, W. Pegios, C. McMahon, J. Balzer, J. Waitzinger, G. Pirovano and J. Lissuer, *Am. J. Roentgenol., 158* (1992) 887.
35 O. Clément, Mühler, A. Vexler, Y. Bertheźene and R.C. Brasch, *Invest. Radiol., 27* (1992) 612.
36 G. Schuhmann-Giampieri, H. Schmitt-Willich, W. Press, C. Negishi, H. Weinmann and U. Speck, *Radiology, 183* (1992) 59.
37 M. Saeed, M.F. Wendland, E. Tomei, S.M. Rocklage, S.C. Quay, M.E. Moseley, C. Wolfe and C.B. Higgins, *Radiology, 173* (1989) 763.
38 B.R. Rosen, J.W. Belliveau and D. Chien, *Magn. Res. Q., 5* (1989) 263.
39 H. Sakuma, M. O'Sullivan, J. Lucas, M.F. Wendland, M. Saeed, M.C. Dulce, K.L. Krayl, A. Watson and C.B. Higgins, *J. Magn. Res. Imaging, 3(P)* (1993) 37.
40 I.H. Cox, L.M. Prayer, M.E. Moseley, J. Kucharczyk, W.P Dillon, K. Bleyl and A. Watson, *J. Magn. Res. Imaging, 3(P)* (1993) 42.
41 J.F. Desreux, E. Merciny and M.F. Loncin, *Inorg. Chem., 20* (1981) 987.
42 R.M. Clay, S. Corr, M. Micheloni and P. Paoletti, *Inorg. Chem., 24* (1985) 3330.
43 J.F. Desreux and P.P. Bartholmy, *Int. J. Rad. Appl. Instrum. [B], 15* (1988) 9.
44 J.F. Desreux and M.-F. Loncin, *Inorg. Chem., 25* (1986) 69.
45 M.-R. Spirlet, J. Rebizant, J.F. Desreux and M-F. Loncin, *Inorg. Chem., 23* (1984) 359.
46 G. Gaughan, in V.M. Runge *et al.* (eds.), *Enhanced Magnetic Resonance Imaging*, C.V. Mosby, St. Louis, MO, 1989.
47 M.F. Tweedle, G.T. Gaughan and J.H. Hagan, *US Patent 4,885,363,* granted 12/23/87 (E.R. Squibb).
48 W.D. Horrocks and D.R. Sudnick, *J. Am. Chem. Soc., 101* (1979) 334.